

## Video Processing for Pipeline Inspection by Endoscopy

Nafaa NACEREDDINE<sup>1</sup>, Aissa BOULMERKA<sup>2</sup>, Nadia MHAMDA<sup>1</sup>

<sup>1</sup> Reseach Center in Industrial Technologies CRTI  
Algiers, Algeria ; e-mail: [n.nacereddine@crti.dz](mailto:n.nacereddine@crti.dz), [n.mhamda@crti.dz](mailto:n.mhamda@crti.dz)

<sup>2</sup> DMI, Centre Universitaire de Mila  
Mila, Algeria; e-mail: [a.boulmerka@centre-univ-mila.dz](mailto:a.boulmerka@centre-univ-mila.dz)

### Abstract

Because of the increasing requirements in regards to the pipeline transport regulations, the operators take care to the rigorous application of checking routines that ensure nonoccurrence of leaks and failures. In situ pipe inspection systems such as endoscopy, remains a reliable mean to diagnose possible abnormalities in the interior of a pipe such as corrosion. Through digital video processing, the acquired videos and images are analyzed and interpreted to detect the damaged and the risky pipeline areas.

Thus, the objective of this work is to bring a powerful analysis tool for a rigorous pipeline inspection through the implementation of specific algorithms dedicated to this application for a precise delimitation of the defective zones and a reliable interpretation of the defect implicated, in spite of the drastic conditions inherent to the evolution of the endoscope inside the pipeline and the quality of the acquired images and videos.

**Keywords:** Pipeline, inspection, motorized engine, video/image processing, corrosion detection/interpretation

## 1. Introduction

The pipelines are most likely to be attacked by corrosion, cracking or manufacturing defect, resulting sometimes in catastrophic damage (human damage, environmental pollution, additional repair costs, extended pumping shutdown, etc.). Consequently, the operators ensure rigorous monitoring schedule to prevent occurrence of any breakdown due to fluid leaks. Nowadays, such a situation poses increasingly severe requirements in terms of rules and standards governing the fluid pipe transport.

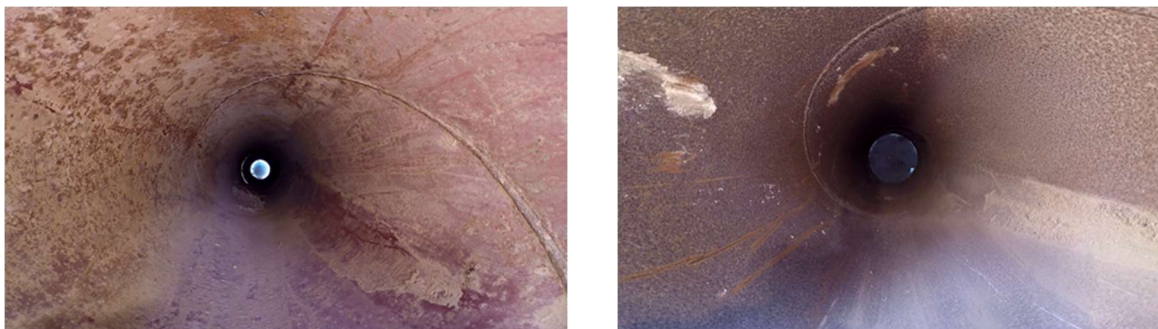


**Figure 1. Examples of pipeline internal views**

For the purpose mentioned above, in situ pipe inspection systems such as endoscopy, remains a reliable mean to diagnose possible abnormalities in the interior of a pipe such as corrosion. The latter is defined as the breaking down or destruction of material, especially a metal through oxidation or chemical reactions [1]. The corrosion attacks remain the principal cause of fluid leaks and pipeline breaks.

In this work, the endoscope consists in a motorized engine equipped with a digital camera. The recovered videos and images inside the inspected pipelines are analyzed and interpreted using

digital video processing to detect the damaged and risky areas such as cracks, corrosion, lack of thickness, etc. To this end, the main stages of this work consist in:

- 1) Designing and conceiving an automated motorized engine with embedded camera where the control is insured by Field Programmable Gate Arrays (FPGA) technology, and
- 2) Implementing image/video processing and analysis software for an accurate detection and reliable identification and interpretation of the defective or risky areas such corrosion, found inside the pipeline.

## 2. Motorized Vehicle Setup

For the realized pipeline endoscope called “Pipe Explorer”, the stepper motors driving the wheels are controlled by Zedboard (Xilinx Zynq-7000) FPGA card while the embedded CCD camera acquiring the videos is controlled by MicroZed FPGA card.

The endoscope is composed of:

- 4 wheels
- 4 stepper motors (1.8°/step) rotating on 360°.
- 4 drivers microstep (JK 1545), DC power input type: 24V~50VDC. Output current: 1.3A-4.5A.
- 1 EPL camera USB with 2 megapixel of resolution.
- Lighting sources through 12 LEDs (12V) Samsung.
- 3 Lead batteries rechargeable of capacity 12V/9Ah each, for the motors supply.
- 2 Lithium batteries of capacity 12V/11Ah each, to supply Zedboard and MicroZed cards.
- 1 Lithium battery 12v/11A to supply the LEDs.

For the endoscope thus realized as shown in Fig. 2, the following characteristics are noted:

- Dimensions : 30cm × 33cm × 54 cm
- Weight : 25 kg
- Autonomy: 6 hours for a run of 2 km.



Figure 2. The endoscope "Pipe-Explorer".

## 3. Video Analysis Software

### 3.1. Context

In the context of pipeline inspection by endoscopy, we have developed software including video processing and analysis techniques in order to interpret the acquired videos.

It is a question here of videos acquired inside the water transportation pipelines which, after a certain time of service, are prone to different types of attacks and degradations, particularly, corrosion. It is thus important to determine its localization, its extent and its degree of severity in order to take appropriate corrective action.

Since the corroded part changes its appearance with respect to the rest of the pipeline, the images constituting the video sequence must be exploited using image segmentation techniques in order to extract the object representing corrosion, i.e. the defective area, from the background representing the undamaged region of the pipe.

In fact, the segmentation constitutes one of the most significant problems in the image analysis system, because the result obtained at the end of this stage strongly governs the final quality of interpretation [2]. Color is a distinctive parameter that can be used to extract the corroded area from the rest of the internal pipeline view. Since these color images can be converted into grayscale images, thresholding techniques become a strong candidate for efficient segmentation.

Thresholding is the process of partitioning pixels in the images into object and background classes based upon the relationship between the gray level value of a pixel and a parameter called the threshold. Because of their efficiency in performance and their simplicity in theory, thresholding techniques have been studied extensively and a large number of thresholding methods have been published [3] [4].

Generally, for the images obtained from the video sequence acquired inside the pipeline, the overlapping between the corroded region and the background representing the healthy areas is large. This is due to the luminance variability of the corrosion and the background areas, in addition of the presence of artifacts. In such case, by a global thresholding, we do not obtain the desired results. That is why a local adaptive thresholding technique can be employed to overcome the above-mentioned problem. In this paper, the method of Sauvola [5], which is an improved version of the method of Niblack [6], and the method Feng [7], which is an improved version of the method of Wolf [8], are applied to detect in-situ pipeline corrosion and are compared in terms of detection efficiency.

### ***3.2. Color image conversion in grayscale***

A gray level image can be generated from the three channels red, green and blue (RGB) of a color image. This process converts the luminance of each pixel in gray level using a combination of RGB colors where a good grayscale conversion will weight each color based on how the human eye perceives it. A common formula in image processing is given by

$$I_{gr} = 0.30 I_R + 0.59 I_G + 0.11 I_B \quad (1)$$

where,  $I_{gr}$  is the pixel gray level of the grayscale image and  $I_R$ ,  $I_G$  and  $I_B$  are the pixel values of the color image in red, green and blue channels, respectively.

### ***3.3. Image thresholding***

In locally adaptive thresholding, the threshold value  $T(x,y)$  is computed on the neighborhood of the current pixel  $(x,y)$ , i.e.

$$b(x,y) = \begin{cases} 0 & \text{if } f(x,y) < T(x,y) \\ 1 & \text{otherwise} \end{cases} \quad (2)$$

where,  $f$  is the input grayscale image and  $b$  is the output binary image.

### 3.3.1. Sauvola thresholding method

The main idea of Niblack's thresholding method [6] is to vary the threshold value, for each pixel  $(x,y)$ , over the input image of size  $(M \times N)$ , based on the local mean  $\mu(x,y)$  and the local standard deviation  $\sigma(x,y)$  in a  $W \times W$  window centered around the pixel  $(x,y)$ . The threshold value at pixel  $(x,y)$  is computed by  $T(x,y) = \mu(x,y) + k\sigma(x,y)$  where,  $k$  is a parameter which depends on image content. The parameters  $W$  and  $k$  are chosen empirically. This method tends to produce a big amount of noise, particularly, when the image background contains light textures, which are considered as object with small contrast. To overcome the above mentioned problems, Sauvola et al. [5] proposed an improved formula to compute the threshold

$$T(x,y) = \mu(x,y) \left( 1 - k \left( 1 - \frac{\sigma(x,y)}{R} \right) \right) \quad (3)$$

where  $R$  is the dynamic range of standard deviation and  $k$  a parameter which takes positive values in the range  $[0.2 \ 0.5]$ .

In this method, the parameter  $k$  controls the value of the threshold in the local window such that the higher the value of  $k$ , the lower the threshold from the local mean  $\mu(x,y)$  [9].

### 3.3.2. Feng thresholding method

Feng's thresholding method [7] is improved from Wolf et al. [8] thresholding approach in order to tolerate different degrees of illumination unevenness. This method uses two local windows: a primary and a secondary window with the former contained within the latter. The values of local mean  $\mu(x,y)$ , local standard deviation  $\sigma(x,y)$  and minimum gray level  $M$ , are calculated in the primary local window and the dynamic range of standard deviation  $R_\sigma$  is calculated in the secondary larger window. The threshold value  $T(x,y)$  in a local window is obtained from:

$$T(x,y) = (1 - \alpha_1) \times \mu(x,y) + \alpha_2 \times \left( \frac{\sigma(x,y)}{R_\sigma} \right) \times (\mu(x,y) - M) + \alpha_3 M \quad (4)$$

where  $\alpha_2 = k_1 \times (\sigma(x,y)/R_\sigma)^\gamma$ ,  $\alpha_3 = k_2 \times (\sigma(x,y)/R_\sigma)^\gamma$ , and  $\alpha_1$ ,  $\gamma$ ,  $k_1$  and  $k_2$  are positive constants.  $\gamma$  is set to 2 and  $\alpha_1$ ,  $k_1$  and  $k_2$  are in the ranges of  $[0.1 \ 0.2]$ ,  $[0.15 \ 0.25]$ ,  $[0.01 \ 0.05]$ , respectively.

### 3.3.3. Algorithms complexity:

In order to compute the threshold  $T(x,y)$ , local mean and standard deviation have to be computed for each pixel. Computing  $\mu(x,y)$  and  $\sigma(x,y)$  in a direct way results in a computational complexity of  $O(W^2NM)$  for an  $M \times N$  image. In order to speed up the computation, an efficient way of computing local means and variances using sum tables (integral images) is proposed in [10] [11] so that the computational complexity does not depend on the window dimension anymore, reducing thus, the computational complexity from  $O(W^2M \times N)$  to  $O(M \times N)$ .

Indeed, for our application which deals with online pipeline inspection, it is important to speed-up the image and video analysis algorithms since slow inspection systems lead to extended pumping downtime where, the cost incurred through lost production would be dramatic. So, the use of integral image in this paper permits to the corrosion detection process based on Niblack, Sauvola and Feng thresholding methods to be faster since less downtime means more working time and then, more benefits.

## 4. Experiments

### 4.1. Software interface presentation

We have developed software dedicated to the detection of corrosion where an interactive interface, illustrated in Fig. 3, permits to (1) load the video of our interest, (2) choose the size of the adaptive thresholding window  $W$ , (3) choose the values of Sauvola and Feng methods parameters  $k$ ,  $R$ ,  $\alpha_1$ ,  $\gamma$ ,  $k_1$ ,  $k_2$  and  $R_\sigma$  and (4) finally choose the number of the frames to be processed from the whole video sequence.

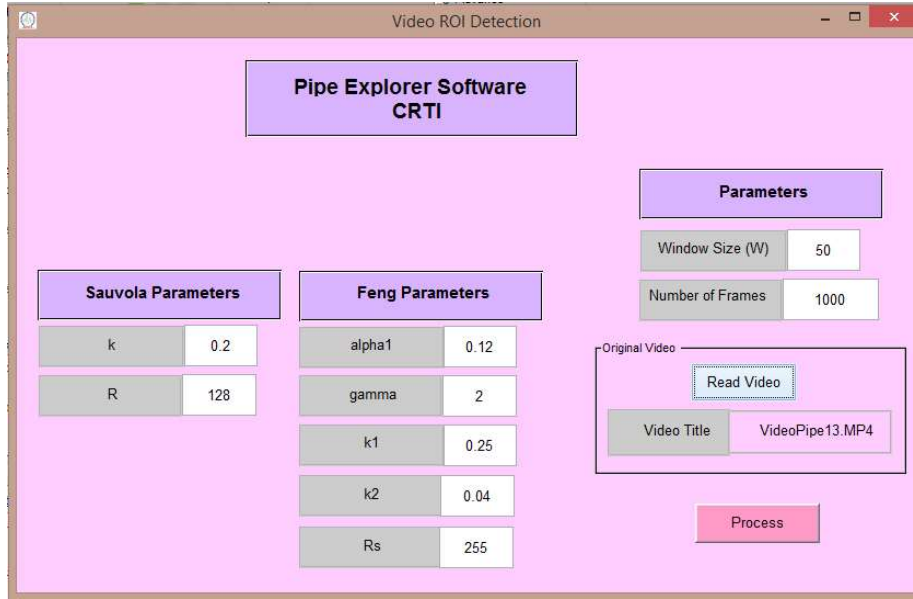


Figure 3. Presentation of the “Pipe Explorer Software” interface

Before displaying the segmented frames for both methods, a procedure of processing removal on the area surrounding the disk image, representing the deep internal view of the pipeline, is applied (see blue circle in Fig. 4). The processing removal in this area is motivated by the fact that the latter looks very dark since it is very far from the embedded camera and the lighting reaching it is low. Furthermore, the considered regions are gradually processed as the motorized vehicle progresses in the pipeline.

### 4.2. Region uniformity measure

The uniformity of a feature over a region is inversely proportional to the variance of the values of that feature evaluated at every pixel belonging to that region [12]. In this paper, the region uniformity measure  $U$ , used to evaluate the segmentation method performance, is given by

$$U = 1 - \frac{w_0\sigma_0^2 + w_1\sigma_1^2}{\sigma_{\max}^2} \quad (5)$$

where  $(\pi_0, \sigma_0^2)$  and  $(\pi_1, \sigma_1^2)$  are the (area ratio, variance) of the foreground and the background regions, respectively; whilst  $\sigma_{\max}^2$  is the maximum image variance given by  $(f_{\max} - f_{\min})^2/2$ . The highest (near to 1) is the value of  $U$ , the highest is the thresholding quality.

### 4.3. Results and discussion

For the test, we have chosen a video sequence obtained by the embedded camera, composed of 1000 frames and stored on a section of water transport pipeline presenting localized attacks of corrosion. The red spots displayed on the output frames representing the risky areas are obtained by Sauvola and Feng thresholding methods. As example, the results for frame 66 are illustrated in Fig. 4. The comparison between the methods of Sauvola and Feng in terms of proportion of damaged areas and thresholding evaluation based region uniformity measure, for all the 1000 images composing the acquired video sequence, are provided by the graphs of Fig. 5.a and Fig 5.b, respectively.

It appears from both pictures and graphics that the Sauvola method slightly under-segments the input image compared to the Feng method as shown in Fig. 4 where visually, some parts of the defect indications are missed in the case of Sauvola thresholding. This can be confirmed by the measure of the proportions of the damaged region area (colored in red) in regards of the whole processed input image for Sauvola and Feng methods, which are about 5.1% and 10.3%, respectively. The case of frame 66 is valid for all the frames of the video sequence where, the damaged region percentages vary, for Sauvola, in the range of [1.6% 9.8%] with an average of 6.2% whereas, it varies, for Feng, in the range of [5.4% 16.2%] with an average of 12%. Regarding the thresholding performance evaluation, the average values of uniformity measure, on all the video frames, is slightly better for Feng ( $U \approx 0.960$ ) than for Sauvola ( $U \approx 0.958$ ).

It is worth to note a possible presence of false positive indications which overestimate the corrosion such as the spiral welding joint in Fig. 4. That said, it is imperative to compare these results with those obtained by an expert for their validation and in order to guide the choice of the thresholding parameters.

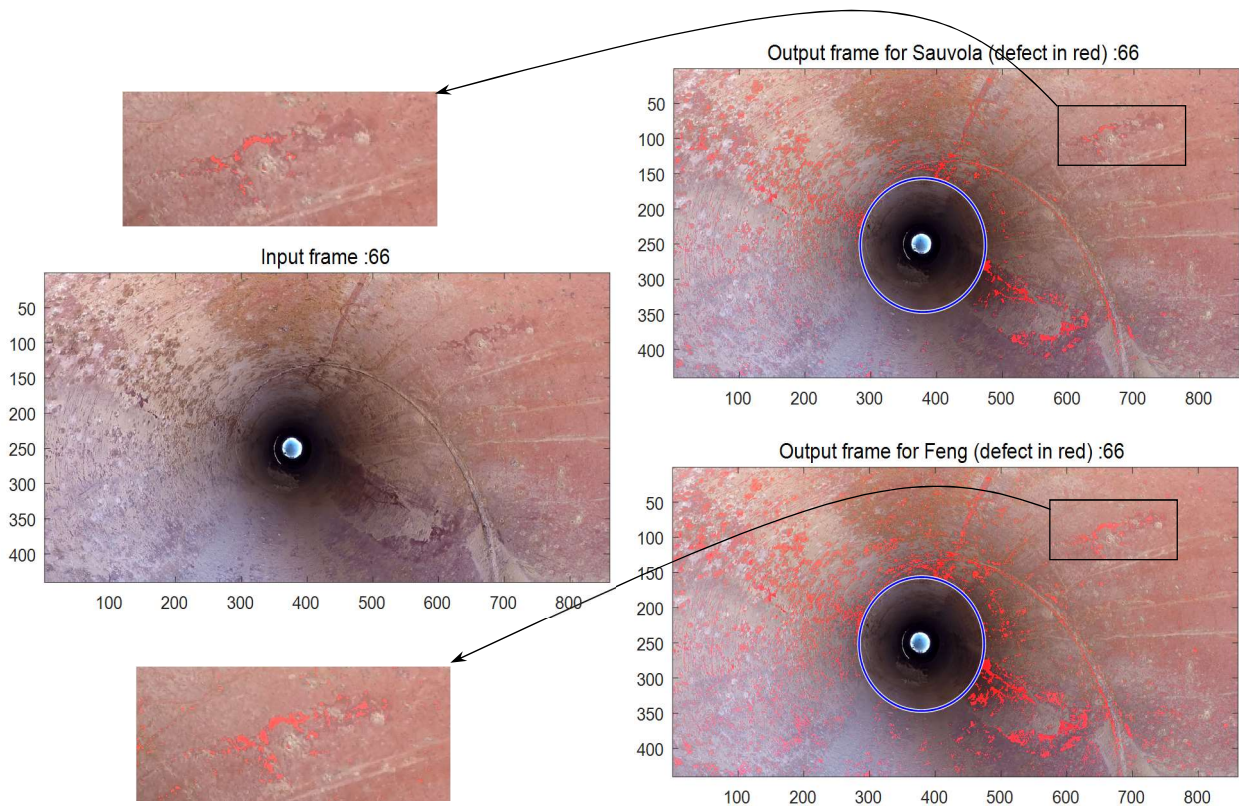
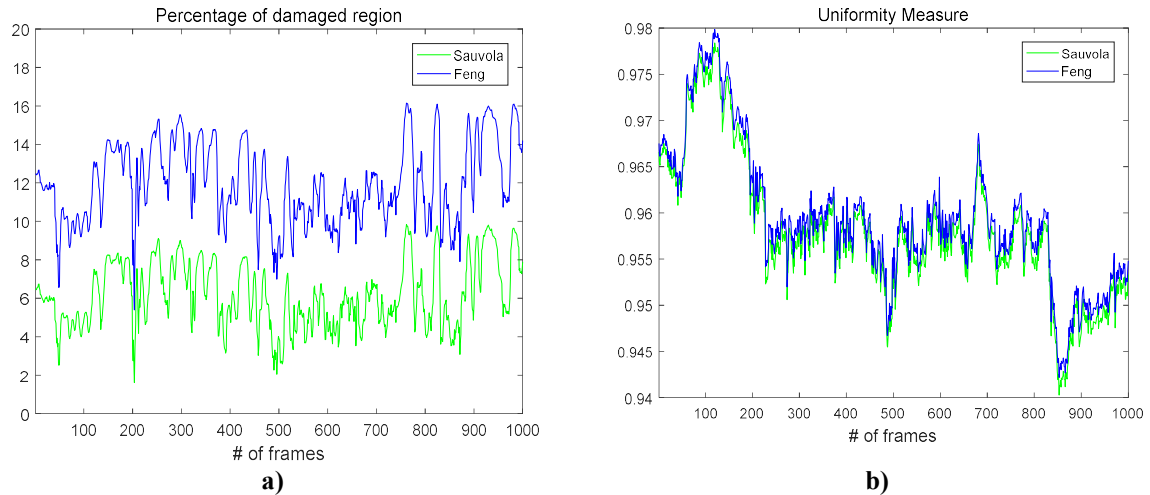


Figure 4. Sauvola and Feng thresholding results for frame 66



**Figure 5. a) Percentage of damaged region areas and b) uniformity measures for methods of Sauvola and Feng on the whole video sequence**

## 5. Conclusion

In this paper, a modern visual equipment “Endoscope” to inspect the interior part of the pipe is used. It consists in a motorized engine embedding a CCD camera. Here, the endoscope is controlled using FPGA technology. A video sequence acquired from a water transport pipeline, presenting mainly corrosion indications, is analyzed and interpreted.

Through dedicated software, the indications of corrosion are extracted using two image thresholding methods: Sauvola and Feng. The results are then quantified in terms of area ratio of possible damaged region and in terms of thresholding evaluation measures. To conclude, it reveals from the results that the complex nature of such images requires to the image and video processing techniques to be evaluated in a supervised manner, i.e. by using a ground truth provided by an expert. In other words, a realistic corrosion detection and interpretation should take into account *a priori* knowledge on the objects composing the internal view of a pipeline such as welding joint, land deposit, stones, stains and soils, which could drastically influence the final interpretation results. These last remarks will be deeply investigated in future works.

## Acknowledgements

This research was supported by CRTI as part of technological development of research products with a socio-economic impact. We thank all the team members of project “Pipeline Inspection by Endoscopy” who have participated in the realization of the “Endoscope” which make possible the acquiring of video sequences in pipeline and then their processing: the subject of the study in this paper.

## References

1. The free dictionary by Farlex. <http://www.thefreedictionary.com/corrosion>.
2. Soler L., G. Malandrin, H. Delingnette, “Segmentation automatique: Application aux angioscanners 3D”, *Revue de Traitement de signal*, Vol. 15, 1998.
3. Lee S. U., S. Y. Chung, R. H. Park, “A comparative performance study of several global thresholding techniques for segmentation”, *Computer Vision, Graphics, and Image Processing*, Vol. 52, pp. 171–190, 1990.
4. Sezgin M., B. Sankur, “Survey over image thresholding techniques and quantitative performance evaluation”, *Journal of Electronic imaging*, Vol. 13, No 1, pp. 146–165, 2004.
5. Sauvola J., M. Pietikainen, “Adaptive document image binarization”, *Pattern Recognition*, Vol. 33, No 2, pp. 225–236, 2000.
6. Niblack W., “Introduction to digital image processing”. Prentice Hall, 1986.
7. Feng M. L., Y. P. Tan, “Contrast adaptive binarization of low quality document images”, *IEICE Electronics Express*, Vol 1, No 16, pp. 501–506, 2004.
8. Wolf C., J. M. Jolion, “Extraction and recognition of artificial text in multimedia documents”, *Pattern Analysis and Applications*, Vol. 6, No 4, pp. 309–326, 2004.
9. Shafait F., D. Keysers, T.M. Breuel, “Efficient implementation of local adaptive thresholding techniques using integral images”, *Document Recognition and Retrieval XV*, Proc. SPIE 6815, San Jose, CA, 2008.
10. Crow F, “Summed-area tables for texture mapping”, *ACM SIGGRAPH Comput. Graph.*, Vol. 18, pp. 207–212, 1984.
11. Viola P., M. Jones, “Rapid Object Detection using a Boosted Cascade of Simple Features”, *Proceedings of the IEEE Computer Society Conference on Computer Vision and Pattern Recognition*, Kauai, HI, USA, pp. 511–518, 8–14 December 2001.
12. Levine M. D., A. M. Nazif, “Dynamic Measurement of Computer Generated Image Segmentations”, *IEEE Transactions on Pattern Analysis and Machine Intelligence*, Vol. 7, No 2, pp. 155-164, 1985.